Received: 26 November 2021 | Revised: 16 March 2022 | Accepted: 12 April 2022

DOI: 10.1002/pip.3567

RESEARCH ARTICLE

PROGRESS IN PHOTOVOLTAICS WILEY

Analysis of the degradation of amorphous silicon-based modules after 11 years of exposure by means of IEC60891:2021 procedure 3

Michel Piliougine[1] | Paula Sánchez-Friera[2] | Giovanni Petrone[1] | Francisco José Sánchez-Pacheco[3] | Giovanni Spagnuolo[1] | Mariano Sidrach-de-Cardona[4]

[1]Dipartimento di Ingegneria dell'Informazione ed Elettrica e Matematica Applicata/DIEM, Università degli Studi di Salerno, Fisciano, Salerno, Italy

[2]Solar PV Consultancy Services, Solkeys, Gijón, Spain

[3]Departamento de Tecnología Electrónica, Universidad de Málaga, Málaga, Spain

[4]Departamento de Física Aplicada II, Universidad de Málaga, Málaga, Spain

Correspondence
Michel Piliougine, Dipartimento di Ingegneria dell'Informazione ed Elettrica e Matematica Applicata/DIEM – Università degli Studi di Salerno. Via Giovanni Paolo II 132. 84084 Fisciano (SA), Italy.
Email: mpiliouginerocha@unisa.it

Funding information
Ministero dell'Istruzione, dell'Università e della Ricerca, Grant/Award Numbers: PRIN2020-HOTSPHOT 2020LB9TBC, PRIN2017-HEROGRIDS 2017WA5ZT3_003; Università degli Studi di Salerno, Grant/Award Number: FARB Funds; Ministerio de Ciencia, Innovación y Universidades, Grant/Award Number: RTI2018-095097-B-I0

Abstract

The degradation of two amorphous silicon-based photovoltaic (PV) modules, namely, of single junction amorphous silicon (a-Si) and of micromorph tandem (a-Si/μ-Si), after 11 years of exposure in the south of Spain is analyzed. Their *I-V* curves were measured outdoors to study the changes of the electrical parameters in the course of three different periods: during the initial days of exposure, during the first year, and in the subsequent 10-year period. The translation of the curves to an identical set of operating conditions, which enables a meaningful comparison, was done by the different correction procedures described in the standard IEC60891:2021, including the *procedure 3*, which does not require the knowledge of module parameters, whose values are typically not available. The annual power degradation rates over the entire 11-year period are 1.12% for the a-Si module, which is 3.02% for the first year, and 0.98% for the a-Si/μ-Si, which is 2.29% for the initial year.

KEYWORDS
amorphous silicon, IEC60891, *I-V* curve correction, microcrystalline silicon, outdoor measurement, photovoltaic degradation, thin film

1 | INTRODUCTION

Amorphous silicon thin-film PV modules offer an alternative to well-established crystalline silicon PV (c-Si), with potentially lower manufacturing costs, reduced energy pay-back time, lower weight, and optimal suitability to special applications, for example, building integrated PV.[1] This technology offers a good performance under cloudy skies, high operating temperatures, or partial-shading conditions.[2] Although other thin-film technologies, such as CdTe or CIGS, also provide those advantages over c-Si without implying a strong decrement of the performance, amorphous-based technologies are still a profitable option because they use materials very abundant and nontoxic.[3]

Degradation processes of amorphous silicon PV modules have been analyzed in many papers available in the literature.[4–20] The dispersion of the degradation rates documented by different authors is significantly wider than the dispersion observed on crystalline PV modules, even though there are comparatively many more works

TABLE 1 Selection of works about degradation of amorphous silicon based PV modules showing type of load, months of exposure and determined annual degradation rates for maximum power

Authors	Months	Load	Climate	%/year
Single junction amorphous silicon				
Adelstein and Sekulic[5]	72	inv	BSk	1.0
Adelstein and Sekulic6, [6]	60	inv	BSk	1.7
Cassini et al.7, [7]	15	inv	BSh	5.5
Gottschalg et al.9, [9]	52	–	Cfb	1.3
Kichou et al.[11]	42	inv	Csa	2.3
Kyprianou et al.12, [12]	96	inv	Csa	1.4
Makrides et al.[14]	60	inv	Csa	1.9
Sharma et al.16, [16]	28	inv	BSh	6.4
Silvestre et al.[17]	60	–	Bsk	2.3
Singh et al.[18]	36	–	BSh	1.3
Ye et al.[20]	36	mpp	Af	2.0
Tandem amorphous silicon/microcrystalline silicon				
Aarich et al.[4]	32	inv	BSh	1.5
Ferrada et al.[8]	16	inv	BWk	3.9
Kichou et al.[10]	42	inv	Csa	2.2
Limmanee et al.[13]	48	inv	Aw	1.8–2.1
Ozden et al.[15]	48	inv	Csb	1.9
Silvestre et al.[17]	60	–	BSk	2.7
Tahri et al.[19]	36	–	BSk	1.7

Note: inv (within an array connected to an inverter); mpp (alone biased to its maximum power point); – (not specified by the authors).

addressing the degradation of the latter family of technology, as shown in the comprehensive review conducted by Jordan et al,[21] stating a range box for the long-term annual degradation rate of amorphous based modules manufactured in the last decade between 0.8 and 2%/year.[21] A summary of annual degradation rates, in terms of power, reported in recent articles can be found in Table 1. The column titled **Climate** expresses the climatic conditions under which the PV modules have been exposed in each cited work, using the Köppen–Geiger index.[22]

Further research is required to gain a deeper knowledge about the degradation of amorphous silicon-based modules; this will allow to reduce the uncertainty affecting the estimations of the energy delivered by PV plants based on this technology. As it can be argued from Table 1, single junction amorphous silicon commonly shows degradation rates in the range of 2.0±0.3% per year,[6,11,14,17,20] although lower[6,9,12,18] and higher values[7,16] are reported, reaching even more than 6%/year. In general, a similar dispersion is found for the degradation rates estimated for micromorph modules and also similar or slightly lower values,[4,8,10,13,15,17,19] with a maximum rate around 4%/year.

In this paper, the performance of two modules is analyzed. The first module is a single-junction hydrogenated amorphous silicon (a-Si:H) module manufactured by Kaneka and with a nameplate stabilized efficiency of 6.3%.[23] The second one is a micromorph tandem a-Si/μ-Si module with a nameplate stabilized efficiency of 8.5%.[24] Both PV modules were exposed to sunlight for the first time in 2010 and have been exposed outdoors for a period over 11 years without any electric load connected to their terminals. It should be noted that degradation is also dependent on the type of the load and degradation analyses at module level are often conducted with no load for practical reasons.[9,17–19] The dependence of the degradation of a-Si modules on the type of load was investigated by Fanni et al,[25] which observed higher degradation rates for modules under open-circuit conditions.[25]

The study carried on over these thin-film modules has been divided into three different parts: (1) the initial strong power drop during the first days of exposure is analyzed; (2) the degradation during the first 12 months is studied; (3) finally, a comparison of the module performance before and after the subsequent 10 years of exposure is performed.

These technologies usually show a significant initial degradation due to the Staebler–Wronski effect.[26] Therefore, it is common to expose the modules outdoors for an initial stabilization period prior to the start of the monitoring campaign. The stabilization period for a-Si is typically considered to be of about 6 weeks.[27–29] Other studies report longer periods (one year or more) for a complete stabilization.[10,30,31] Hence, the rates obtained for the first and second analyses, which refer to the first days and to the first year, are affected to some extent by stabilization issues, being only the results of the third analysis representative of the long-term degradation.

This paper relies on a previous study of degradation of PV modules from the same authors,[32] and it is based on the same measurement system. In this paper, a novel translation method has been employed to correct the *I-V* curves to reference conditions for determining the parameter variation. Most of the translation methods available in literature, including procedures 1, 2, and 4 of IEC60891:2021,[33] require, in addition to the temperature coefficients, which are provided by the manufacturers for new nondegraded PV modules, some additional parameters, which are normally not available in the specifications. Table 4 shows a small survey of some of these methods of correction of *I-V* curves, providing the parameters required by each one and their meanings. Although IEC60891:2021 also describes methods to estimate such parameters, these tasks require many additional *I-V* curve measurements, which are usually difficult to be performed without a solar simulator. In this paper, the required corrections are performed by using the *procedure 3* of the standard IEC60891:2021. It is an algorithm requiring only a minimum of three measured *I-V* curves, and no internal parameter or temperature coefficients. Moreover, some experiments show that this interpolation procedure provides much better results than the other ones.[34] Finally, instead of assuming the Standard Test Condition (STC) as reference, the measurements are translated to values of irradiance and cell temperature that are closer to the actual ones, so that the errors added by the correction procedure are minimized. As it has been done in few papers up to now,[35–37] in this paper it has been considered the following set of operating conditions: $G = 800$ W/m^2 and $T_{cell} = 35$ °C. Ad hoc irradiance and cell temperature defined by the user is

usually referred as Alternate Reporting Condition (ARC). This paper is organized as follows: Section 2 describes the measurement system and procedures, with a special focus on the *I-V* curve correction procedure 3 of IEC60891:2021. Section 3 shows the results and plots obtained by the application of the proposed methodology. In Section 4, a comparative analysis and a discussion are presented. The main conclusions of the study are summarized in Section 5.

2 | METHODOLOGY

2.1 | Experimental set-up

The modules were exposed on the roof of *School of Computer and Telecommunication Engineering* of the *University of Málaga*. According to the Köppen–Geiger classification,[22] Málaga (Spain) belongs to the **Csa** region (Mediterranean climate), such as the references[11,12,14] in Table 1. They were installed on a tilted metallic structure next to other PV modules used in other studies. Additional details about the emplacement can be found in King et al.[32] Except than during the short time during which the modules were connected to the curve tracer, both modules operated in V_{OC} condition.

Some papers in the literature[38,39] show the use of commercial field curve tracers based on a capacitive load. As for the study of degradation for the first days of exposure, this type of measurement system has been used, that is, the *PVPM 6020C* from the manufacturer *Photovoltaik Engineering*.[40] However, curve tracers of this type do not have enough accuracy for individual PV modules and they can only get very few *I-V* samples around I_{SC}. This last problem is due to the fact that the charging of a capacitor is very fast at the beginning (when crossing the $V = 0$ V axis), in such a way the A/D converters to capture the points of the curve do not have time to acquire enough points. Therefore, for the rest of the measurements, an experimental *I-V* curve tracer made up of different laboratory instruments has been used. It includes a bipolar power supply and a pair of multimeters from the manufacturers *Kepco* and *Agilent* respectively, controlled through a custom software[41,42] running on a PC. This type of power supply allows to control the voltage sweeping time by software, so that it is possible to obtain as many points as you want around I_{SC}. This system is referred in the rest of the paper as *Kepco/Agilent*, and the same used in 2017 in King et al,[32] except for the pyranometer; indeed, for the experiments described in this paper, a Kipp & Zonen CM-21[43] has been used.

Table 2 shows the features of the single-junction amorphous silicon module[23] and of the tandem of amorphous silicon/microcrystalline silicon module.[24] The symbols α, β, and γ stand for the temperature coefficients of I_{SC}, V_{OC}, and P_{max}, respectively, whereas η is the nameplate efficiency and N_s is the number of cells.

Careful attention must be paid to the spectrum when characterizing a-Si modules outdoors, because they have a narrow spectral response. King et al[31] assume for this technology a variation of the performance around a 7% due to spectral changes. Therefore, to obtain realistic degradation rates the indicators to be compared should be estimated under similar spectral conditions, for example, by performing the measurement under clear skies in the same week of different years. To ensure a high spectral similarity, it is possible to compare the *I-V* curves using the average photon energy (APE),[44,45] which can be calculated from the solar spectrum. In this paper, the latter one has been measured by an EKO MS-710[46] on the module plane, by using the range (350–1050) nm to integrate the APE. Therefore, for every *I-V* curve, a reading of the APE value is available, having this parameter a strong dependency on the solar position, the season of the year, and the level of temperature, humidity and clouding.[45]

Each PV module under study has been tested by five sets of measurements taken during different selected days from the exposure period, which are labeled as *a*, *b*, *c*, *d*, and *e*, as it can be seen in Table 3. The measurement tests identified by *a* and *b* were performed using the *PVPM 6020C*, whereas *c*, *d*, and *e* were made with the *Kepco/Agilent* system. Measurements were acquired under clear-sky days after a careful cleaning of each module surface and irradiance sensors. During each experiment, the system acquired some *I-V* curves of each module, and then three *I-V* curves at an irradiance greater than 600 W/m^2 is identified.

Finally, over these three selected curves, the *procedure 3* of the *IEC60891:2021*[33] has been applied to obtain a new calculated curve referred to the ARC condition, which has been defined in this paper as 800 W/m^2 of irradiance and 35°C of cell temperature. By comparing the corrected curves of *a* and *b*, the degradation of the initial 9-day exposure period is estimated, whereas by performing the same procedure with the pairs (*c*,*d*) and (*d*,*e*), the degradation during the 1-year and the 10-year periods are determined.

2.2 | *Procedure 3* of *IEC 60891:2021*

The International Standard IEC 60891:2021[33] describes four procedures aimed at estimating the *I-V* curve of a PV device under conditions of irradiance and temperature different than those under which they were measured. The main disadvantage of the *procedures 1*, *2*,

TABLE 2 Specifications at STC of the PV modules under study

Manufacturer/model	Tech.	N_s	P_{max} W	I_{SC} A	V_{OC} V	I_{Pmax} A	V_{Pmax} V	α %/°C	β %/°C	γ %/°C	η %
Kaneka/GEA-060	a-Si:H	108	60	1.19	92	0.90	67	+0.075	−0.305	−0.23	6.3
Phoenix Solar/PHX-120-LV	a-Si/μ-Si	96	121	3.34	59.20	2.69	45.00	+0.07	−0.30	−0.24	8.51

TABLE 3 History of the modules and different measuring points with accumulated exposure time

Test	Date	Description	Total exposure time	
–	26th-Mar-2010	Installation of the modules		
a	29th-Mar-2010	First measurement with *PVE PVPM*	3 days	9 days
b	7th-Apr-2010	Second measurement with *PVE PVPM*	12 days	
–	12th-Apr-2010	Uninstalling and storing in dark room		
–	29th-Oct-2010	Reinstalling of the modules		
c	2nd-Nov-2010	First measurement with *Kepco/Agilent*	3 weeks	1 year
d	29th-Oct-2011	Second measurement with *Kepco/Agilent*	1 year and 3 weeks	10 years
e	28th-Oct-2021	Third measurement with *Kepco/Agilent*	11 years and 3 weeks	

and 4, in the same Standard is that they require to know beforehand several additional parameters. Some of them are temperature coefficients that can be found in the specification sheets of the PV modules, but referred to new as-built PV modules (hence not necessarily applicable to degraded specimens as it is our case[32]). Moreover, some require parameters that are hardly available and that must be determined by additional sets of measurements. Although IEC 60891:2021[33] provides the guidelines to determine all these parameters, the procedures are difficult to implement in outdoor conditions. On the other hand, *procedure 3* does not require any temperature coefficient or internal parameter. It is based only on data from three measured *I-V* curves:

- *Curve 1*: $(V_1[i], I_1[i])$, where $i = 1,\ldots,n_1$, measured at an irradiance G_1 and a cell temperature T_1.
- *Curve 2*: $(V_2[j], I_2[j])$, where $j = 1,\ldots,n_2$, measured at an irradiance G_2 and a cell temperature T_2.
- *Curve 3*: $(V_3[k], I_3[k])$, where $k = 1,\ldots,n_3$, measured at an irradiance G_3 and a cell temperature T_3.

The problem consists in determining, from these three curves, a new *Curve 0* given by $(V_0[i], I_0[i])$ which corresponds to the target conditions G_0 and T_0. An interpolation is conducted using an auxiliary *Curve 4* as an intermediate step, which corresponds to the operating conditions G_4 and T_4. As first, *Curve 4* is obtained from *Curve 1* and *Curve 2*; then, afterwards, *Curve 3* and *Curve 4* are used to estimate the final *Curve 0*. The interpolation is first done in the irradiance/temperature plane, as shown in Figure 1, and then completed in the voltage/current space by using the same parameters, as explained below. The values G_4 and T_4 are defined as linear combinations of G_1 and G_2, and T_1 and T_2 respectively, as shown in Equations (1) and (2), where ω is a parameter to be determined. The target irradiance G_0 and temperature T_0 are estimated from G_3 and G_4, and T_3 and T_4, respectively, using another unknown parameter ϕ, as shown in Equations (3) and (4). This leads to a system of 4 equations and four unknowns (G_4, T_4, ω, and ϕ).

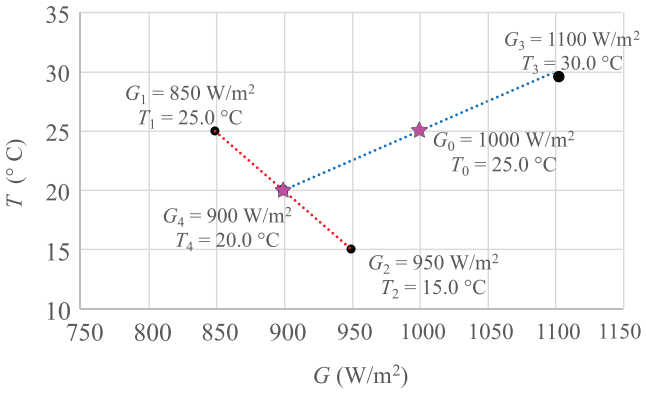

FIGURE 1 *The operating conditions of curves 1, 2, and 3* (black dots) are interpolated to obtain the operating conditions of Curves 4 and 0 (magenta stars)

$$G_4 = G_1 + \omega \cdot (G_2 - G_1), \tag{1}$$

$$T_4 = T_1 + \omega \cdot (T_2 - T_1), \tag{2}$$

$$G_0 = G_3 + \phi \cdot (G_4 - G_3), \tag{3}$$

$$T_0 = T_3 + \phi \cdot (T_4 - T_3). \tag{4}$$

The set of equations defined in the standard has been simplified by defining a new translation parameter $\psi = \omega \cdot \phi$ and by substituting the values of G_4 and T_4 in Equations (3) and (4). This leads to Equations (5) and (6), which are easily solved by Equation (7). In the case of the example of Figure 1, the solution is ϕ=0.5 and ψ=0.25, and then $\omega = \psi/\phi$= 0.5.

$$G_0 - G_3 = (G_1 - G_3) \cdot \phi + (G_2 - G_1) \cdot \psi, \tag{5}$$

$$T_0 - T_3 = (T_1 - T_3) \cdot \phi + (T_2 - T_1) \cdot \psi, \tag{6}$$

$$\mathbf{A} = \begin{bmatrix} G_1 - G_3 & G_2 - G_1 \\ T_1 - T_3 & T_2 - T_1 \end{bmatrix},$$
$$\mathbf{X} = \begin{bmatrix} \phi \\ \psi \end{bmatrix}, \quad (7)$$
$$\mathbf{B} = \begin{bmatrix} G_0 - G_3 \\ T_0 - T_3 \end{bmatrix} \Rightarrow \mathbf{A}\cdot\mathbf{X} = \mathbf{B} \Rightarrow \mathbf{X} = \mathbf{A}^{-1}\cdot\mathbf{B}.$$

The next step is aimed at obtaining the *I-V* curves. It has been assumed that I_{SC1} and I_{SC2} are the short-circuit currents of *Curve 1* and *Curve 2*, respectively. For each point of *Curve 1* $(V_1[i], I_1[i])$, its partner $(V_2[j], I_2[j])$ is sought in *Curve 2* so that the following condition is fulfilled: $I_2[j] - I_1[i] = I_{SC2} - I_{SC1}$. Then, a new point $(V_4[i], I_4[i])$ of *Curve 4* is obtained by applying Equations (8) and (9). Analogously, for each point of *Curve 3* $(V_3[i], I_3[i])$, the best matching point $(V_4[j], I_4[j])$ of *Curve 4* is selected satisfying $I_4[j] - I_3[i] = I_{SC4} - I_{SC3}$, and the point $(V_0[i], I_0[i])$ of *Curve 0* is generated by means of Equations (10) and (11). Figure 2i,ii sketches this point-by-point process to obtain the auxiliary *Curve 4* and the final corrected *Curve 0*, respectively.

$$V_4[i] = V_1[i] + \omega\cdot(V_1[i] - V_2[j]), \quad (8)$$

$$I_4[i] = I_1[i] + \omega\cdot(I_1[i] - I_2[j]), \quad (9)$$

$$V_0[i] = V_3[i] + \phi\cdot(V_3[i] - V_4[j]), \quad (10)$$

$$I_0[i] = I_3[i] + \phi\cdot(I_3[i] - I_4[j]). \quad (11)$$

2.3 | Alternative correction procedures

Although the study presented in this paper is based on the *Procedure 3* of IEC 60891:2021, only for comparative purposes, the degradation rates of both PV modules have also been estimated using other two approaches described in the same standard, in addition to the simplest possible method as described by Smith et al.[47] (only requiring the three temperature coefficients α, β, and γ). Table 4 provides a brief summary of some of these correction methods.

Contrary to *Procedure 3*, which requires three initial measured curves, all these other approaches use as start point only one measurement under the initial conditions noted as (G_1, T_1). From the initial set of *I-V* points, these methods can be used to estimate $I_{SC,2}$ and $V_{OC,2}$, and $P_{max,2}$ at the target conditions (G_2, T_2).

Due to the fact that these formulas require to know the value of several parameters, although some of them could be provided by the manufacturer, in this work all these coefficients have been determined experimentally using the guides given by IEC 60891:2021[33] and other useful recommendations.[32] However, in this paper, this process is not explained, reporting only the final values of these coefficients for a new module (a nondegraded one) of each type (see Table 5). Finally, although in the literature there are approaches to perform a correction by the angle of incident (see the Sandia Performance Model[49]), we have not applied this type of correction to our measurements.

3 | RESULTS

Each measured *I-V* curve is associated to a row in Table 6, whose identifier Mxn $= \langle (K|P)(a|b|c|d|e)(1|2|3) \rangle$ refers to the module (*K*: Kaneka / *P*: Phoenix Solar), the measurement point (noted in Table 3 as *a*, *b*, *c*, *d*, and *e*), and the selected measured curve (with the subfixes

TABLE 4 Methods of correction of *I-V* curves to different conditions of irradiance and temperature

Method	Reference	Required parameters[a]
Simple Method	Smith et al.[47]	$\alpha_{rel}, \beta_{rel}, \gamma_{rel}$
Anderson's Method	Anderson[48]	$\alpha_{rel}, \beta_{rel}, \gamma_{rel}, \delta_{rel}$
IEC 60891:2021 *proc. 1*	IEC 60891[33]	$\alpha, \beta, R_s, \kappa$
IEC 60891:2021 *proc. 2*	IEC 60891[33]	$\alpha_{rel}, \beta_{rel}, R_s, \kappa, B_1, B_2$
IEC 60891:2021 *proc. 3*	IEC 60891[33]	None
IEC 60891:2021 *proc. 4*	IEC 60891[33]	$\alpha_{rel}, R_s, \varepsilon$

[a]Meaning of the parameters:
- α: Variation of I_{SC} respect to device temperature.
- α_{rel}: Relative variation of I_{SC} respect to device temperature.
- β: Variation of V_{OC} respect to device temperature.
- β_{rel}: Relative variation of V_{OC} respect to device temperature.
- γ_{rel}: Relative variation of P_{max} respect to cell temperature.
- R_S: internal series resistance of the device.
- κ: Variation of R_S respect to device temperature.
- δ: Irradiance correction factor of V_{OC} (quadratic fit).
- B_1, B_2: Irradiance correction factors of V_{OC} (quadratic fit).
- ε: Material parameter dependent on the bandgap energy and the diode factor.

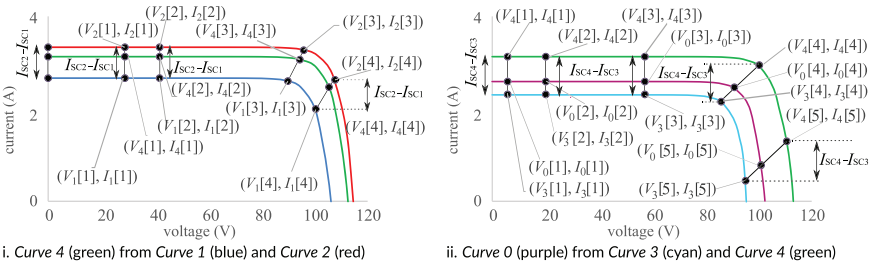

i. *Curve 4* (green) from *Curve 1* (blue) and *Curve 2* (red)

ii. *Curve 0* (purple) from *Curve 3* (cyan) and *Curve 4* (green)

FIGURE 2 Two interpolations to obtain the corrected *Curve 0* from 3 measured curves and the auxiliary *Curve 4*

TABLE 5 Values of the required parameters

	Kaneka	Phoenix Solar
α [A/°C]	+0.0009	+0.0021
α_{rel} [1/°C]	+0.00073	+0.00069
β [V/°C]	−0.283	−0.214
β_{rel} [1/°C]	−0.0030	−0.0036
γ [W/°C]	−0.15	−0.39
γ_{rel} [1/°C]	−0.0021	−0.0033
$R_{S,STC}$ [Ω]	5.66	0.406
κ [Ω/° C]	−0.056	+0.0028
δ [−]	0.198	0.055
B_1 [−]	0.007	0.043
B_2 [−]	0.797	0.053

1, *2*, or *3*). Each final corrected curve (the auxiliary curves have not been included) has also its row in Table 6 marked in bold and with the subfix 0 (e.g., **Ka0** or **Pa0**). As it can be seen, instead of using STC as reference, we have defined our own ARC conditions: 800 W/m^2 of irradiance on module plane and 35°C of cell temperature (values selected based on a rough estimation trying to minimize the gap to correct).

In addition to the main electrical parameters of each curve (calculated using the approach given by Emery[50]), the value of APE, estimated from the measured spectrum, is provided (see Piliougine et al[45] for the details). Table 7 shows the monthly average value of APE obtained from spectral measurements acquired in Málaga from January 2011 to December 2011 for clear-sky days and irradiance values $G \geq 600$ W/m^2. As it can be seen, the measurement points *c*, *d*, and *e* in Table 6 are characterized by APE values approximately ranging between 1.871 and 1.894 eV, which fit well to the mean values for October, November, and December in Table 7. Great care should be taken when comparing measurements taken in different periods of the year because there could be important spectral variations.

By taking into account that the measurement tests *a* and *b* have been performed by the curve tracer *PVPM* and the other ones by the *Kepco/Agilent* system, it has been decided to avoid comparing these different sets of measurements when estimating degradation rates. For example, when comparing in Table 6 the corrected curves **Kb0** and **Kc0**, P_{max} and I_{SC} are greater in the last curve, but this is due to the use of two different measurement systems. In other words, to calculate degradation rates, we must compare measurements performed using the same equipment.

To illustrate the IEC60891:2021 *procedure 3*, for each module and set of measurements a plot in Figure 3 or Figure 4 shows in black the three selected *I-V* curves of the same day used as input, and in blue the corrected curve. The most relevant electrical points of each curve, measured or corrected, are also pointed out with a star.

All the plots in Figure 3 are related to measurements performed by the *PVPM* curve tracer. Besides the low accuracy of this system for characterizing single PV modules, the high level of noise around the open-circuit point is very significant, and also the lack of measured points near to the short-circuit condition. Figure 4 shows measurements acquired with the *Kepco/Agilent* system, with a better distribution of points that allows good estimations of P_{max}, I_{SC}, and V_{OC}. From our experience, *procedure 3* of IEC60891:2021 is very sensitive to noise, due to the propagation of the error of the three measured curves to the corrected one.

4 | DISCUSSION

Having estimations of each electrical parameter at the different measurement points of 2010, 2011, and 2021, it is possible to determine the respective degradation rates: (1) for the initial 9 days of exposure; (2) for the following 12 months; (3) for the next 10 years; (4) and finally an annual degradation rate for the entire period of 11 years.

Several facts should be highlighted from these results. Because they are modules based on amorphous silicon, during the initial exposure they experiment a very strong degradation. Only during the first days the a-Si module experiments a power drop close to 6%, due to the Staebler–Wronski effect.[26,51] However, for the a-Si/μ-Si case, this effect is lower, although it is also very significant (around 4%) taking into account that only 9 days of exposure have been considered. These initial drops have not been included in the estimation of the following rates.

Regarding the other electrical parameters during this initial period, both modules have similar behaviors in I_{SC}: A significant drop of 2.4% for the a-Si specimen and of 3% for the a-Si/μ-Si case. On the other hand, the drop in terms of V_{OC} is significantly lower (around 0.7 in both modules). This suggests that the initial drop during the first hours of exposure is related to a decrease of the current flow through the cells. Another difference between both specimens is the evolution of the FF: whereas the drop in the micromorph case is insignificant, for the single junction amorphous it is close to 2.7%, also dragging the value of V_{Pmax}.

When analyzing the 1-year period (between Nov-2010 and Nov-2011), it is possible to see a strong decrease of the I_{SC}: around 2% in the a-Si module whereas the drop for the a-Si/μ-Si module is much lower (0.73%/year). However the degradation of V_{OC} is almost insignificant in the case of the amorphous module but strong enough in the micromorph case. Despite the strong drop of the FF for the initial days in the a-Si module, the degradation of this indicator during the 1-year period seems to be significantly lower. For the micromorph module, the behavior is more stable.

Focusing on the degradation in terms of power for both modules during the entire first year, the single junction amorphous module has degraded a bit more than 3.02% whereas the micromorph module has experienced an annual power drop close to 2.29%. In both cases, these rates are in agreement to those summarized in Table 1, except for those works[7,16] where the period of study is relatively short (30 months or less). This fact suggests that studies on amorphous silicon technologies require long exposure periods of several years in order to overpass stabilization and obtain realistic degradation rates. Therefore, the most interesting analysis of this paper is the estimation

TABLE 6 List of measured and corrected *I-V* curves of each PV module

Id.	Date	UTC	G W/m^2	T_{cell} °C	APE eV	P_{max} W	I_{SC} A	V_{OC} V	I_{Pmax} A	V_{Pmax} V	FF %
Ka1	29th-Mar-2010	09:12	623	31.9	1.886	40.8	0.717	88.58	0.594	68.60	64.2
Ka2	29th-Mar-2010	09:45	733	40.9	1.891	47.8	0.859	86.91	0.715	66.86	64.0
Ka3	29th-Mar-2010	10:45	896	42.2	1.901	58.5	1.052	87.40	0.876	66.81	63.7
Ka0	**29th-Mar-2010**		**800**	**35.0**		**52.3**	**0.929**	**88.72**	**0.770**	**67.90**	**63.4**
Kb1	7th-Apr-2010	09:37	718	46.2	1.886	42.8	0.819	84.54	0.619	64.09	61.9
Kb2	7th-Apr-2010	09:58	785	44.7	1.891	47.3	0.898	85.36	0.734	64.45	61.7
Kb3	7th-Apr-2010	10:40	890	50.2	1.872	53.5	1.029	84.51	0.844	63.39	61.5
Kb0	**7th-Apr-2010**		**800**	**35.0**		**49.3**	**0.907**	**88.12**	**0.737**	**66.92**	**61.7**
Kc1	2nd-Nov-2010	09:44	683	36.5	1.881	38.7	0.787	83.10	0.625	61.96	59.2
Kc2	2nd-Nov-2010	11:47	893	35.2	1.886	50.4	1.013	84.71	0.806	62.60	58.8
Kc3	2nd-Nov-2010	12:29	864	38.9	1.888	48.2	0.980	83.52	0.778	61.93	58.9
Kc0	**2nd-Nov-2010**		**800**	**35.0**		**46.3**	**0.932**	**84.26**	**0.741**	**62.54**	**59.0**
Kd1	29th-Oct-2011	09:21	633	29.3	1.885	35.0	0.709	84.13	0.561	62.38	58.7
Kd2	29th-Oct-2011	09:36	679	31.3	1.886	37.2	0.763	83.28	0.603	61.69	58.5
Kd3	29th-Oct-2011	10:06	755	33.7	1.890	41.9	0.857	83.73	0.678	61.86	58.3
Kd0	**29th-Oct-2011**		**800**	**35.0**		**44.9**	**0.914**	**84.05**	**0.723**	**62.12**	**58.5**
Ke1	28th-Oct-2021	12:51	841	45.3	1.890	43.1	0.972	78.71	0.757	56.87	56.4
Ke2	28th-Oct-2021	13:51	742	44.7	1.886	38.0	0.854	78.48	0.666	57.08	56.7
Ke3	28th-Oct-2021	14:41	610	41.1	1.877	31.1	0.694	78.47	0.541	57.41	57.1
Ke0	**28th-Oct-2021**		**800**	**35.0**		**40.6**	**0.909**	**79.96**	**0.708**	**57.34**	**55.9**
Pa1	29th-Mar-2010	09:18	645	38.1	1.889	77.7	2.213	56.67	1.766	44.03	64.9
Pa2	29th-Mar-2010	09:42	722	45.5	1.891	86.2	2.401	55.81	1.999	43.11	64.3
Pa3	29th-Mar-2010	10:27	864	49.0	1.905	103.4	2.906	55.69	2.421	42.70	63.9
Pa0	**29th-Mar-2010**		**800**	**35.0**		**96.9**	**2.647**	**57.54**	**2.197**	**44.12**	**63.6**
Pb1	7th-Apr-2010	09:19	640	44.8	1.882	72.7	2.123	54.33	1.749	41.57	63.0
Pb2	7th-Apr-2010	09:55	774	42.4	1.887	87.8	2.509	55.67	2.060	42.62	62.9
Pb3	7th-Apr-2010	11:52	995	51.9	1.896	112.3	3.298	54.87	2.703	41.56	62.1
Pb0	**7th-Apr-2010**		**800**	**35.0**		**93.0**	**2.568**	**57.13**	**2.109**	**44.11**	**63.4**
Pc1	2nd-Nov-2010	09:47	701	38.1	1.883	79.39	2.321	55.52	1.872	42.42	61.6
Pc2	2nd-Nov-2010	11:50	885	39.5	1.893	101.8	2.974	55.95	2.397	42.47	61.2
Pc3	2nd-Nov-2010	12:41	859	40.8	1.887	98.4	2.895	55.53	2.332	42.19	61.2
Pc0	**2nd-Nov-2010**		**800**	**35.0**		**91.6**	**2.608**	**57.14**	**2.106**	**43.50**	**61.5**
Pd1	29th-Oct-2011	09:20	631	29.6	1.885	68.9	2.041	56.20	1.630	42.27	60.1
Pd2	29th-Oct-2011	10:00	743	34.1	1.892	81.9	2.447	55.92	1.954	41.93	59.9
Pd3	29th-Oct-2011	10:16	774	35.6	1.894	85.5	2.571	55.78	2.055	41.60	59.6
Pd0	**29th-Oct-2011**		**800**	**35.0**		**89.5**	**2.589**	**56.09**	**2.063**	**43.36**	**61.6**
Pe1	28th-Oct-2021	10:01	705	44.6	1.872	75.1	2.344	53.86	1.835	40.92	59.5
Pe2	28th-Oct-2021	12:01	859	48.3	1.871	91.8	2.890	53.86	2.259	40.63	59.0
Pe3	28th-Oct-2021	13:51	744	44.7	1.879	79.1	2.470	53.93	1.934	40.88	59.3
Pe0	**28th-Oct-2021**		**800**	**35.0**		**81.7**	**2.514**	**54.86**	**1.969**	**41.49**	**59.2**

of the annual degradation rates by comparing the measurements before and after the 10-year period (or 11-year period if the first year is also included).

By comparing the measurement points *d* and *e*, the power degradation rates in both cases are similar to those obtained for crystalline silicon that are installed in the same site and by using the same measurement equipment.[52] However, whereas in that case the long-term degradation was characterized by a strong decrease of I_{SC}, in the case of the a-Si module the annual drop of current can be neglected, and for the a-Si/μ-Si module it is very low as well. In other words, whereas

TABLE 7 Monthly averaged values of APE (eV) for $G \geq 600$ W/m^2 in Málaga (data from 2011)

APE	Jan.	Feb.	Mar.	Apr.	May.	Jun.	Jul.	Aug.	Sep.	Oct.	Nov.	Dec.
(eV)	1.870	1.884	1.888	1.897	1.904	1.908	1.908	1.907	1.902	1.892	1.878	1.872

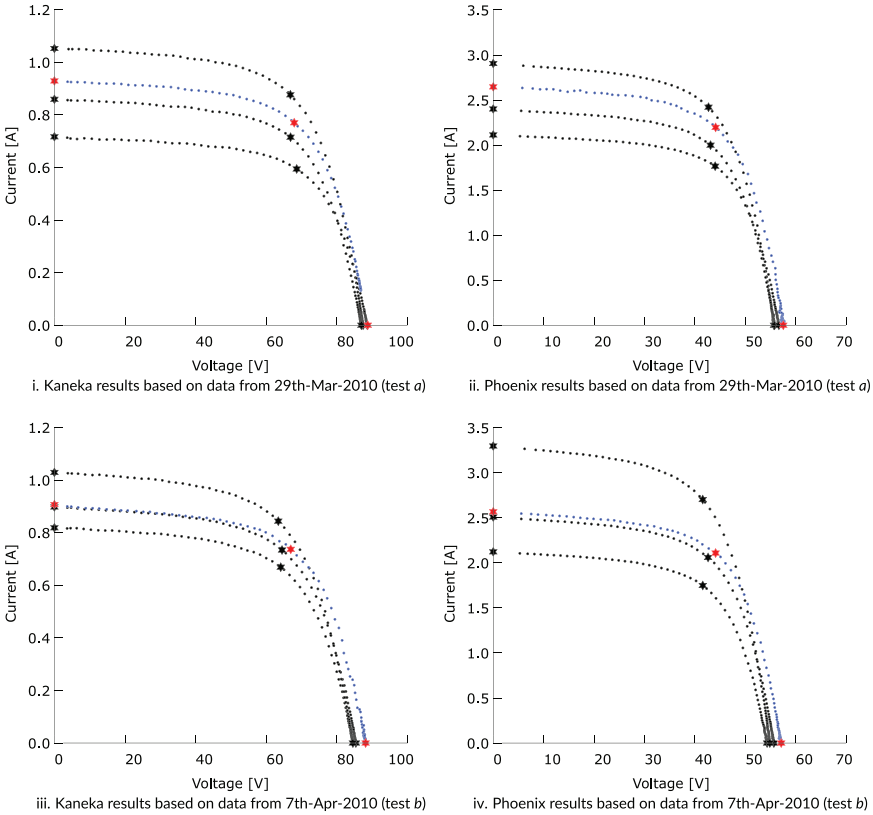

FIGURE 3 Measured (black) and corrected (blue) curves for both PV modules and tests *a* and *b* (*PVPM*)

in the infancy of amorphous Si-based modules the degradation is mainly due a decrease of the current, as the samples age, it is the reduction in voltage that dominates the long-term degradation. In addition, the long-term annual degradation rate for FF (around 0.4% for both cases) is very significant in comparison to the one shown in Piliougine et al[32] and referring to mono-crystalline silicon modules, which is negligible.

The last column of Table 8 shows the degradation rates for the entire period of 11 years, including the first year of exposure. The power degradation rate for the a-Si module is 1.12%/year. By comparing this value with the results reported in Table 1, it emerges that it is in good agreement with several literature achievements.[9,12,18] On the other hand, the a-Si/μ-Si module has experienced a degradation in terms power of 0.98%, that is a bit lower than the rates reported in the literature.

Finally, the alternative methods which could be used to correct *I-V* curves and listed in Table 4 have been tested, but *IEC 60891:2021 procedure 4* has been excluded because a specific value of ε is not available. For the sake of brevity, the comparative has been only performed for the degradation rate of the maximum power P_{max}, as it can be seen in Table 9.

For the single amorphous module, if only the initial period of exposure is analyzed, the procedures 1 and 2 of the *IEC 60891:2021* are in agreement with the obtained results by the chosen method, whereas the other two approaches overestimate a bit this initial degradation in terms of power. A better agreement is achieved between all the methodologies in the case of the micromorph module. However, much stronger differences between the correction methods are found when analyzing the other periods of exposure. During the first year, for the a-Si module, only *IEC 60891:2021 proc. 1* has obtained a result similar to *IEC 60891:2021 proc. 3*. On the other hand, for the a-Si/μ-Si module, all the methods seem to overestimate the degradation in terms of power. For long-term degradation, there is also no agreement between the different approaches. From the results of this comparative, we must conclude, as other authors have stated in the literature,[53] that there is a dependence of the estimated degradation rate on the method of correction used, and this fact requires further study. One possible reason are the high uncertainty associated to the determination of the required parameters to apply some of these methods,[54] specially if their determination is performed based on outdoor measurements.

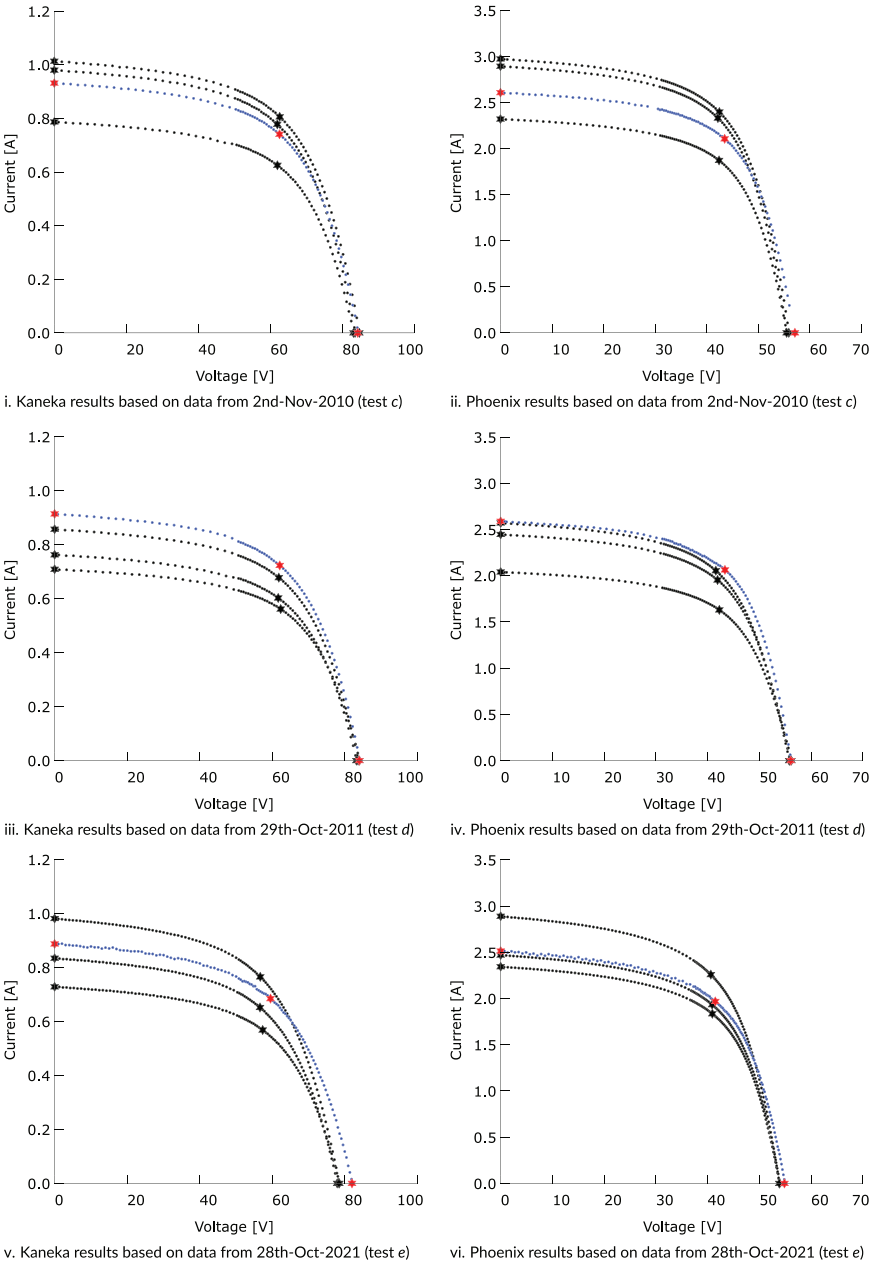

i. Kaneka results based on data from 2nd-Nov-2010 (test *c*)

ii. Phoenix results based on data from 2nd-Nov-2010 (test *c*)

iii. Kaneka results based on data from 29th-Oct-2011 (test *d*)

iv. Phoenix results based on data from 29th-Oct-2011 (test *d*)

v. Kaneka results based on data from 28th-Oct-2021 (test *e*)

vi. Phoenix results based on data from 28th-Oct-2021 (test *e*)

FIGURE 4 Measured (black) and corrected (blue) curves for both PV modules and tests *c*, *d*, and *e* (*Kepco/Agilent*)

TABLE 8 Degradation rates for each module considering different periods of time

	Kaneka a-Si				*Phoenix Solar* a-Si/μ-Si			
	a* vs. *b **(9 days)**	***c* vs. *d*** **(1 year)**	***d* vs. *e*** **(10 years)**	***c* vs. *e*** **(11 years)**	***a* vs. *b*** **(9 days)**	***c* vs. *d*** **(1 year)**	***d* vs. *e*** **(10 years)**	***c* vs. *e*** **(11 years)**
IEC 60891:2021 Procedure 3								
P_{max} (W)	5.74%	3.02%/y	0.96%/y	1.12%/y	4.02%	2.29%/y	0.87%/y	0.98%/y
I_{SC} (A)	2.37%	1.93%/y	0.05%/y	0.22%/y	2.98%	0.73%/y	0.29%/y	0.33%/y
V_{OC} (V)	0.68%	0.25%/y	0.49%/y	0.46%/y	0.71%	1.84%/y	0.22%/y	0.36%/y
I_{Pmax} (A)	4.29%	2.43%/y	0.21%/y	0.40%/y	4.01%	2.04%/y	0.46%/y	0.59%/y
V_{Pmax} (V)	1.44%	0.68%/y	0.77%/y	0.76%/y	≈0%/y	0.32%/y	0.43%/y	0.42%/y
FF (%)	2.68%	0.85%/y	0.44%/y	0.48%/y	0.31%	0.32%/y	0.39%/y	0.34%/y

TABLE 9 Comparative of power degradation rates for each module using alternative methods of correction

	Kaneka a-Si				*Phoenix Solar* a-Si/μ-Si			
	a vs. *b* (9 days)	*c* vs. *d* (1 year)	*d* vs. *e* (10 years)	*c* vs. *e* (11 years)	*a* vs. *b* (9 days)	*c* vs. *d* (1 year)	*d* vs. *e* (10 years)	*c* vs. *e* (11 years)
Simple method								
P_{max} (W)	6.89%	2.48%/y	0.23%/y	0.43%/y	4.71%	7.24%/y	0.30%/y	0.94%/y
Anderson's method								
P_{max} (W)	6.47%	4.34%/y	0.54%/y	0.86%/y	4.55%	5.44%/y	0.30%/y	0.51%/y
IEC 60891:2021 Procedure 1								
P_{max} (W)	5.82%	3.26%/y	0.43%/y	0.68%/y	4.05%	6.13%/y	0.36%/y	0.43%/y
IEC 60891:2021 Procedure 2								
P_{max} (W)	5.92%	7.06%/y	1.02%/y	1.51%/y	4.49%	4.57%/y	0.32%/y	0.71%/y

In any case, in order to identify the most suitable correction procedure to be used when estimating degradation rates, it is necessary to perform a detailed comparative study among all the several approaches published in the literature, even testing them with modules of different technologies. This can be done using each correcting method to translate an initial measured curve to the conditions of another target curve, also measured, and comparing the corrected curve to the measured target one. Some preliminary experiments in this line have been done in our laboratory, in such away, we can forward that *IEC 60891:2021 proc. 3* outperforms significantly all the other alternatives, giving a corrected curve almost indistinguishable from the measured one.

In fact, using a test set of 100 measured curves, *IEC 60891:2021 proc. 3* is able to correct the curves with a mean error in P_{max} of only 0.6%, whereas *proc. 1* and *proc. 2* have errors of 1.9% and 1.8%, respectively (the other two methods have error greater than 2% when correcting P_{max}). However, this issue is out of the scope of this paper and deserves to be analyzed in detail in a future publication.

5 | CONCLUSIONS

In this paper, the degradation of two amorphous silicon-based PV modules that were exposed in Málaga for 11 years has been analyzed. The *I-V* curves have been measured outdoors by using a suitable measuring system and by converting the selected curves to an identical set of operating conditions by using procedure 3 of the standard *IEC60891:2021*. The calculations described in the standard have been improved by introducing a new equation which makes the computation faster.

The electrical parameters for the same set of operating conditions have been compared at different stages of the exposure period. The obtained degradation rates are in line with those ones reported in the literature. An initial significant degradation, during the first 9 days of exposure, has been observed: this leads to a power decay of 6% and 4% for the single junction a-Si and the micromorph, respectively. The power decay is due to significant ohmic losses and, to a lesser extent, also to losses related to the voltage, together with a significant decrease in FF for the a-Si module. After this initial drop, the FF degradation reduces, but the power decay continues with annual rates of slightly over 3% for the a-Si module and nearly 2.3% for the micromorph module. Finally, for the whole 10-year period, the degradation is dominated by the FF decay, and the annual power degradation rates stabilized to values of nearly 1.0%/year for both modules. These results are not much higher than those ones obtained for crystalline silicon PV modules measured at the same location during the same exposure period. If the first year of exposure is included in our calculus (11-year period), the degradation for the amorphous case is only around 1.12%/year and for the micromorph case around 0.98%/year.

ACKNOWLEDGEMENT

This work is supported by Ministero dell'Istruzione, dell'Università e della Ricerca (Italy) (grant PRIN2020-HOTSPHOT 2020LB9TBC and grant PRIN2017-HEROGRIDS 2017WA5ZT3_003); Università degli Studi di Salerno (FARB funds); Ministerio de Ciencia, Innovación y Universidades (Spain) (grant RTI2018-095097-B-I0).

ORCID

Michel Piliougine https://orcid.org/0000-0002-8169-9727
Paula Sánchez-Friera https://orcid.org/0000-0002-9321-4248
Giovanni Petrone https://orcid.org/0000-0003-0163-9546
Francisco José Sánchez-Pacheco https://orcid.org/0000-0002-0809-8300
Giovanni Spagnuolo https://orcid.org/0000-0002-4817-1138
Mariano Sidrach-de-Cardona https://orcid.org/0000-0002-7030-4232

REFERENCES

1. Dai Y, Bai Y. Performance improvement for building integrated photovoltaics in practice: a review. *Energies*. 2021;14(1):178. https://doi.org/10.3390/en14010178
2. Boxwell M. *Solar Electricity Handbook—2021 Edition: A Simple, Practical Guide to Solar Energy—Designing and Installing Solar PV Systems*. Coventry, UK: Greenstream Publishing Ltd; 2021. https://www.barnesandnoble.com/w/solar-electricity-handbook-2021-edition-michael-boxwell/1138587023

3. Efaz ET, Rhaman MM, Imam SA, et al. A review of primary technologies of thin-film solar cells. *Eng Res Express*. 2021;3(3):32001. https://doi.org/10.1088/2631-8695/ac2353
4. Aarich N, Raoufi M, Bennouna A, Erraissi N. Outdoor comparison of rooftop grid-connected photovoltaic technologies in Marrakech (Morocco). *Energ Build*. 2018;173:138-149. https://doi.org/10.1016/j.enbuild.2018.05.030
5. Adelstein J, Sekulic B. Performance and reliability of a 1–kW amorphous silicon photovoltaic roofing system. In: *31st IEEE Photovoltaic Specialists Conference (PVSC)*. Lake Buena Vista, FL, USA; 2005:1627-1630. https://doi.org/10.1109/PVSC.2005.1488457
6. Adelstein J, Sekulic W. Small PV systems performance evaluation at NREL's outdoor test facility using the PVUSA power rating method. In: *2005 Doe Solar Energy Technologies program Review Meeting*. Denver, CO, USA; 2005:NREL/CP-520-39135. https://www.osti.gov/biblio/882794-small-pv-systems-performance-evaluation-nrel-outdoor-test-facility-using-pvusa-power-rating-method
7. Cassini DA, Costa SCS, Diniz ASAC, Kazmerski LL. Evaluation of failure modes for photovoltaic modules in arid climatic zones in Brazil. In: *48th IEEE Photovoltaic Specialists Conference (PVSC)*; 2021:580-582. https://doi.org/10.1109/PVSC43889.2021.9518798
8. Ferrada P, Araya F, Marzo A, Fuentealba E. Performance analysis of photovoltaic systems of two different technologies in a coastal desert climate zone of Chile. *Sol Energy*. 2015;114:356-363. https://doi.org/10.1016/j.solener.2015.02.009
9. Gottschalg R, Betts TR, Eeles A, Williams SR, Zhu J. Influences on the energy delivery of thin film photovoltaic modules. *Sol Energ Mat Sol C*. 2013;119:169-180. https://doi.org/10.1016/j.solmat.2013.06.011
10. Kichou S, Abaslioglu E, Silvestre S, Nofuentes G, Torres-Ramírez M, Chouder A. Study of degradation and evaluation of model parameters of micromorph silicon photovoltaic modules under outdoor long term exposure in Jaén, Spain. *Energ Convers Manage*. 2016;120:109-119. https://doi.org/10.1016/j.enconman.2016.04.093
11. Kichou S, Silvestre S, Nofuentes G, Torres-Ramírez M, Chouder A, Guasch D. Characterization of degradation and evaluation of model parameters of amorphous silicon photovoltaic modules under outdoor long term exposure. *Energy*. 2016;96:231-241. https://doi.org/10.1016/j.energy.2015.12.054
12. Kyprianou A, Phinikarides A, Makrides G, Georghiou G. Definition and computation of the degradation rates of photovoltaic systems of different technologies with robust principal component analysis. *IEEE J Photovolt*. 2015;5(6):1698-1705. https://doi.org/10.1109/JPHOTOV.2015.2478065
13. Limmanee A, Songtrai S, Udomdachanut N, et al. Degradation analysis of photovoltaic modules under tropical climatic conditions and its impacts on LCOE. *Renew Energ*. 2017;102:199-204. https://doi.org/10.1016/j.renene.2016.10.052
14. Makrides G, Zinsser B, Schubert M, Georghiou G. Performance loss rate of twelve photovoltaic technologies under field conditions using statistical techniques. *Sol Energy*. 2014;103:28-42. https://doi.org/10.1016/j.solener.2014.02.011
15. Ozden T, Akinoglu B, Turan R. Long term outdoor performances of three different on-grid PV arrays in central Anatolia—an extended analysis. *Renew Energ*. 2017;101:182-195. https://doi.org/10.1016/j.renene.2016.08.045
16. Sharma V, Sastry OS, Kumar A, Bora B, Chandel SS. Degradation analysis of a-Si, (HIT) hetro-junction intrinsic thin layer silicon and m-C-Si solar photovoltaic technologies under outdoor conditions. *Energy*. 2014;72:536-546. https://doi.org/10.1016/j.energy.2014.05.078
17. Silvestre S, Kichou S, Guglielminotti L, Nofuentes G, Alonso-Abella M. Degradation analysis of thin film photovoltaic modules under outdoor long term exposure in Spanish continental climate conditions. *Sol Energy*. 2016;139:599-607. https://doi.org/10.1016/j.solener.2016.10.030
18. Singh R, Sharma M, Rawat R, Banerjee C. Field analysis of three different silicon-based technologies in composite climate condition—part II—seasonal assessment and performance degradation rates using statistical tools. *Renew Energ*. 2020;147:2102-2117. https://doi.org/10.1016/j.renene.2019.10.015
19. Tahri A, Silvestre S, Tahri F, Benlebna S, Chouder A. Analysis of thin film photovoltaic modules under outdoor long term exposure in semi-arid climate conditions. *Sol Energy*. 2017;157:587-595. https://doi.org/10.1016/j.solener.2017.08.048
20. Ye J, Reindl T, Aberle A, Walsh T. Performance degradation of various PV module technologies in tropical Singapore. *IEEE J Photovolt*. 2014;4(5):1288-1294. https://doi.org/10.1109/JPHOTOV.2014.2338051
21. Jordan D, Kurtz S, VanSant K, Newmiller J. Compendium of photovoltaic degradation rates. *Prog Photovoltaics*. 2016;24(7):978-989. https://doi.org/10.1002/pip.2744
22. Cui D, Liang S, Wang D, Liu Z. A 1 km global dataset of historical (1979–2013) and future (2020–2100) Köppen–Geiger climate classification and bioclimatic variables. *Earth Syst Sci Data*. 2021;13(11):5087-5114. https://doi.org/10.5194/essd-13-5087-2021
23. Kaneka GEA060 specification sheet. KANEKA; Corporation. https://www.dropbox.com/s/mrr7xm5qeyi1iaf/Kaneka_GEA060.pdf, Last accessed: November 9th, 2021.
24. *Solarmodule Phoenix Solar – PHX – 120 – LV*: Phoenix Solar; AG. https://www.dropbox.com/s/4ohvib18ink1hqa/PhoenixSolar_PHX120LV.pdf, Last accessed: November 9th, 2021.
25. Fanni L, Pola I, Burà E, Friesen T, Chianese D. Investigation of annealing and degradation effects on a-Si PV modules in real operating conditions. In: *24th European Photovoltaic Solar Energy Conference (EU PVSEC)*. Hamburg, Germany; 2009:3596-3599. https://doi.org/10.4229/24thEUPVSEC2009-4AV.3.92
26. Staebler DL, Wronski CR. Reversible conductivity changes in discharge-produced amorphous Si. *Appl Phys Lett*. 1977;31(4):292-294. https://doi.org/10.1063/1.89674
27. *Kaneka Thin Film PV Installation Manual. Module Type: G-EA060*: KANEKA Corporation; 2009. https://www.dropbox.com/s/8n9w6lc077nhcso/KANEKA_MANUAL.pdf, Last accessed: November 9th, 2021.
28. Muñoz-García MA, Marin O, Alonso-García MC, Chenlo F. Characterization of thin film PV modules under standard test conditions: results of indoor and outdoor measurements and the effects of sunlight exposure. *Sol Energy*. 2012;86(10):3049-3056. https://doi.org/10.1016/j.solener.2012.07.015
29. Radue C, Van Dyk EE. A comparison of degradation in three amorphous silicon PV module technologies. *Sol Energ Mat Sol C*. 2010;94(3):617-622. https://doi.org/10.1016/j.solmat.2009.12.009
30. Astawa K, Betts TR, Gottschalg R. Effect of loading on long term performance of single junction amorphous silicon modules. *Sol Energ Mat Sol C*. 2011;95(1):119-122. https://doi.org/10.1016/j.solmat.2010.04.071
31. King DL, Kratochvil JA, Boyson WE. Stabilization and performance characteristics of commercial amorphous–silicon PV modules. In: *28th IEEEE Photovoltaic Specialists Conference (PVSC)*. Anchorage, AK, USA; 2000:1446-1449. https://doi.org/10.1109/PVSC.2000.916165
32. Piliougine M, Oukaja A, Sánchez-Friera P, et al. Analysis of the degradation of single-crystalline silicon modules after 21 years of operation. *Prog Photovoltaics*. 2021;29(8):907-919. https://doi.org/10.1002/pip.3409
33. IEC 60891:2021. *Photovoltaic Devices—Procedures for Temperature and Irradiance Corrections to Measured I-V Characteristics*. 3rd ed. Geneva (Switzerland): International Electrotechnical Commission IEC; 2021. https://webstore.iec.ch/publication/61766
34. Li B, Migan-Dubois A, Delpha C, Diallo D. Evaluation and improvement of IEC 60891 correction methods for I-V curves of defective

photovoltaic panels. *Sol Energy*. 2021;216:225-237. https://doi.org/10.1016/j.solener.2021.01.010
35. Davis KO, Kurtz SR, Jordan DC, Wohlgemuth JH, Sorloaica-Hickman N. Multi-pronged analysis of degradation rates of photovoltaic modules and arrays deployed in Florida. *Prog Photovoltaics*. 2013;21(4):702-712. https://doi.org/10.1002/pip.2154
36. Kumar M, Kumar A, Gupta R. Comparative degradation analysis of different photovoltaic technologies on experimentally simulated water bodies and estimation of evaporation loss reduction. *Prog Photovoltaics*. 2021;29(3):357-378. https://doi.org/10.1002/pip.3370
37. Rawat R, Singh R, Sastry OS, Kaushik SC. Performance evaluation of micromorph based thin film photovoltaic modules in real operating conditions of composite climate. *Energy*. 2017;120:537-548. https://doi.org/10.1016/j.energy.2016.11.105
38. Díez-Suárez AM, de la Calzada-Lorenzo D, González-Martínez A, Álvarez-de Prado L. Thin-film PV modules early degradation analysis: A case study on CIGS. In: *17th International Conference on Renewable Energies and Power Quality (ICREPQ'19)*. Tenerife, Spain; 2019:320-326. https://www.icrepq.com/icrepq19/299-19-diez.pdf
39. Kumar M, Kumar A. Experimental validation of performance and degradation study of canal-top photovoltaic system. *Appl Energ*. 2019;243:102-118. https://doi.org/10.1016/j.apenergy.2019.03.168
40. *Pvpm 2540c/6020c/1000c/1000c40. peak power measuring device and curve tracer for photovoltaic modules*. 1/2009. Iserlohn, Germany: Photovoltaik Engineering GmbH. https://www.dropbox.com/s/j95lesd9h9145eu/pvpm.PDF
41. Piliougine M, Carretero J, Mora-López L, Sidrach-de-Cardona M. Experimental system for current-voltage curve measurement of photovoltaic modules under outdoor conditions. *Prog Photovoltaics*. 2011;19(5):591-602. https://doi.org/10.1002/pip.1073
42. Piliougine M, Carretero J, Mora-López L, Sidrach-de-Cardona M. New software tool to characterize photovoltaic modules from commercial equipment. In: *WEENTECH Proceedings in Energy*; 2018:211-220. https://doi.org/10.32438/WPE.6218
43. *Precision Pyranometer CM21—Instruction Manual*. 304th ed. Delft, Holland: Kipp & Zonen; B.V. https://www.dropbox.com/s/hln7wqhoakb2ax6/KIPPZONEN_cm21.pdf
44. Nofuentes G, Gueymard CA, Aguilera J, Pérez-Godoy MD, Charte F. Is the average photon energy a unique characteristic of the spectral distribution of global irradiance? *Sol Energy*. 2017;149:32-43. https://doi.org/10.1016/j.solener.2017.03.086
45. Piliougine M, Elizondo D, Mora-López L, de Cardona M. Photovoltaic module simulation by neural networks using solar spectral distribution. *Prog Photovoltaics*. 2013;21(5):1222-1235. https://doi.org/10.1002/pip.2209
46. *Eko Grating Spectroradiometer wiser–35750/ms–710/ms–712*. Tokyo, Japan: EKO Instruments Co. Ltd. https://www.dropbox.com/s/t9lo68as2ieawo7/eko.pdf
47. Smith R, Jordan D, Kurtz S. Outdoor PV module degradation of current-voltage parameters. In: *2012 World Renewable Energy Forum National Renewable Energy Laboratory (NREL)*. Denver, CO, USA; 2012:NREL/CP-5200-53713. https://www.osti.gov/biblio/1038302-outdoor-pv-module-degradation-current-voltage-parameters-preprint
48. Anderson AJ. PV translation equations a new approach. *AIP Conf Proc*. 1996;353(1):604-612. https://doi.org/10.1063/1.49391
49. King DL, Boyson WE, Kratochvill JA. Photovoltaic array performance model. SAND2004-3535, Albuquerque,NM, USA, Sandia National Laboratories; 2004. https://doi.org/10.2172/919131
50. Emery K. Photovoltaic calibrations at the National Renewable Energy Laboratory and uncertainty analysis following the ISO 17025 guidelines. NREL/TP-5J00-66873, Golden, CO, USA, National Renewable Energy Laboratory NREL; 2016. https://www.nrel.gov/docs/fy17osti/66873.pdf
51. Yanagisawa T. Long-term degradation tests of amorphous silicon solar cells: correlation between light- and current-induced degradation characteristics. *Microelectron Reliab*. 1995;35(2):183-187. https://doi.org/10.1016/0026-2714(95)90084-4
52. Sánchez-Friera P, Piliougine M, Peláez J, Carretero J, Sidrach-de-Cardona M. Analysis of degradation mechanisms of crystalline silicon PV modules after 12 years of operation in Southern Europe. *Prog Photovoltaics*. 2011;19(6):658-666. https://doi.org/10.1002/pip.1083
53. Phinikarides A, Kindyni N, Makrides G, Georghiou G. Review of photovoltaic degradation rate methodologies. *Renew Sustain Energy Rev*. 2014;40:143-152. https://doi.org/10.1016/j.rser.2014.07.155
54. Piliougine M, Oukaja A, Sidrach-de Cardona M, Spagnuolo G. Temperature coefficients of degraded crystalline silicon photovoltaic modules at outdoor conditions. *Prog Photovoltaics*. 2021;29(5):558-570. https://doi.org/10.1002/pip.3396

How to cite this article: Piliougine M, Sánchez-Friera P, Petrone G, Sánchez-Pacheco FJ, Spagnuolo G, Sidrach-de-Cardona M. Analysis of the degradation of amorphous silicon-based modules after 11 years of exposure by means of IEC60891:2021 procedure 3. *Prog Photovolt Res Appl*. 2022;1-12. doi:10.1002/pip.3567